Guo, Hai and Niu, Jianlei and Morawska, Lidia (2008) *Distribution of respiratory droplets in enclosed environments under different air distribution methods.* Building Simulation: An International Journal , 1(4). pp. 326-335.

Distribution of respiratory droplets in enclosed environments under different air distribution methods

Gao N.P.[1], Niu J.L[2], and L. Morawska[3]
[1]Department of Refrigeration and Thermal Engineering, Tongji University, Shanghai, China Tel: 86-21-65983867 Email: gaonaiping@gmail.com
[2]Department of Building Services Engineering, The Hong Kong Polytechnic University, Hunghom, Kowloon, Hong Kong
[3]School of Physical & Chemical Sciences, Queensland University of Technology, Australia

Abstract
Dispersion characteristics of respiratory droplets in indoor environments are of special interest in controlling transmission of airborne diseases. This study adopts an Eulerian method to investigate the spatial concentration distribution and temporal evolution of exhaled and sneezed/coughed droplets within the range of 1.0~10.0μm in an office room with three air distribution methods, i.e. mixing ventilation (MV), displacement ventilation (DV), and under-floor air distribution (UFAD). The diffusion, gravitational settling, and deposition mechanism of particulate matters are well accounted in the one-way coupling Eulerian approach. The simulation results find that exhaled droplets with diameters up to 10.0μm from normal respiration process are uniformly distributed in MV, while they are trapped in the breathing height by thermal stratifications in DV and UFAD, resulting in a high droplet concentration and a high exposure risk to other occupants. Sneezed/coughed droplets are diluted much slower in DV/UFAD than in MV. Low air speed in the breathing zone in DV/UFAD can lead to prolonged residence of droplets in the breathing zone.

Keywords: Respiratory droplets; air distribution; transmission; airborne disease

Nomenclature

C	Concentration (g/m^3)
$C_{1\varepsilon}$, $C_{2\varepsilon}$, $C_{3\varepsilon}$	constants in the governing equation of ε
C_μ	model constant (=0.0845)
D_p	Brownian diffusivity (m^2/s)
g	gravitational acceleration (m/s^2)
G_B	generation of turbulence kinetic energy due to buoyancy
G_k	generation of turbulence kinetic energy due to the mean velocity gradients

k	turbulent kinetic energy (m^2/s^2)
p	pressure (Pa)
R_ε	strain rate term in the ε equation
S	modulus of the mean rate-of-strain tensor
S_c	source term in the concentration equation
S_{ij}	mean rate-of-strain tensor
S_ϕ	source term of ϕ
t	time (s)
T	temperature (℃)
u	air velocity component in the x direction (m/s)
$\vec{U}$	air velocity vector (m/s)
v	air velocity component in the y direction (m/s)
$\vec{V}_s$	particle settling velocity (m/s)
w	air velocity component in the z direction (m/s)

Greek Symbols

α_k	the inverse effective Prandtl numbers of k equation
α_ε	the inverse effective Prandtl numbers of ε equation
β_T	thermal expansion coefficient (K^{-1})
ε	turbulent kinetic energy dissipation rate (m^2/s^3)
ε_p	particle turbulent diffusivity (m^2/s)
ϕ	a general scalar quantity
μ	molecular viscosity of air (g/ms)
μ_t	turbulent viscosity (g/ms)
μ_{eff}	effective viscosity (g/ms)
ρ	air density (g/m^3)
σ_c	turbulent Prandtl number for concentration
σ_T	turbulent Prandtl number for temperature

Γ_ϕ general form of diffusion coefficients

1. Introduction

Indoor air plays a significant role in airborne infection transmission in many enclosed environments, such as open-plan offices, hospital wards, and commercial aircraft cabins. Virus-containing droplets are disseminated into room air by respiratory activities (talking, coughing, and sneezing), shrink by evaporation, and then are suspended in the air for a prolonged period. Inhalation of the droplet nuclei, which are potentially disease transmission vehicles, may cause infection. A typical airborne infection process is illustrated in Figure 1. In this source-to-receptor relationship, the inhalation intake fraction and dose and the health effect are the two key issues. Intake fraction is defined as the pollutant mass taken in by an exposed person per unit mass produced from a source (Nazaroff 2008). In this frame, risk could be estimated by the product of emission rate, intake fraction, and a health-risk factor.

As illustrated in Figure 1, human exposure, i.e. intake fraction, is closely related to the local concentrations. In many pollution infection risk estimation models, such as the Wells-Riley model, a well-mixing or a uniform concentration field is assumed. However this foundation normally does not exactly hold in practice. Droplet nuclei are carried by convection currents and their concentrations vary in time and space. Infection reports in hospitals, high-rise apartments, offices, and transport vehicles show a close association between airflow pattern and the transmission/spread of infectious diseases (Li et al. 2007), and roughly indicate the role played by different air-distribution methods in the dispersion of virus-containing aerosols. To control or limit spreading by air currents, some certain ventilation systems have been recommended for special occasions, such as CDC guideline for isolation rooms (CDC 1994). For ordinary air-conditioned building rooms, the cool air is usually supplied by mixing ventilation (MV), displacement ventilation (DV), and under-floor air distribution (UFAD). MV aims to create a well-mixing condition and a uniform thermal environment, while DV and UFAD are able to maintain a vertical gradient of temperature and concentration by low-level supply and up-level exhaust. Many studies found DV and UFAD are superior to MV due to their higher pollutant removal effectiveness for non-passive gaseous pollutants. However, their functions in removing expiratory droplets and reducing the risk of indoor cross-infections are less studied so far.

Xie et al. (2007) developed a physical model to quantify the transport distance and evaporation rate of droplets from respiratory activities considering the effect of relative humidity, not indoor airflow pattern. Chao et al. (2008) investigated the movement characteristics of expiratory droplets in a three-bed hospital ward where ventilation air was supplied by two four-way ceiling diffusers and returned through two ceiling exhaust vents. By tracking 10,000 particles, they found that the change in the airflow supply rate had insignificant effect on the transport and deposition of large

droplets (>34μm). But small droplets (<17.5μm) exhibited certain airborne behaviors. Also by Lagrangian approach, Zhu et al. (2006) studied the transport of saliva droplets in a calm indoor space with mixing ventilation which found that droplets from sneezing could travel more than 2m. They concluded that gravity and inertia of small droplets (<30μm) was negligible while droplet of 50~100μm were significantly affected by gravity. In both of these studies, the sneezed droplets exhibited the feature of a high initial momentum and spatial orientation. Lai and Cheng (2007) simulated the expiratory droplets of 0.01μm and 10μm in an empty room occupied by two persons under mixing ventilation and displacement ventilation. In MV, both 0.01μm and 10μm droplets were homogeneously dispersed within a period of around 50s from emission. However, in DV, the dispersion of 10μm droplets was influenced by gravitational settling, showing accumulation of droplets at the lower region near the floor level. Since buoyancy is one of the main driving forces in DV, the relatively weak indoor heat load in Lai and Cheng's study may not capture the typical airflow characteristics in a real displacement ventilated room. Similar studies were carried out by Sun et al. (2007) and Zhao et al. (2005) to investigate the dispersion characteristics in an empty mixing ventilated room. The goal of the present study is to find the performance of MV, DV and UFAD in the transport of bio-aerosols from respiratory activities. Through modeling the droplet concentration distributions using an Eulerian-based model in a real office, the spatial variance of droplet concentrations in steady exhalation conditions and concentration evolution versus time in transient sneezing conditions are described below.

2. Numerical simulations

Cases description

The dimensions of the computational geometry of a hypothetic office room are: 4.0m (length) × 3.0m (width) × 2.7m (height) (Figure 2). Boundary conditions for windows, computer, desk, human body are summarized in Table 1. The heat load in this room approximates 36 W/m^2 (based on floor area). Three air distribution methods, MV, DV, and UFAD, are compared here, and the air supply temperature is 17℃ in MV and 19℃ in DV and UFAD, and the air change rate 5.7 times per hour. The normal components of the inlet air velocity in MV and DV are 2.55m/s and 0.255m/s, respectively. In UFAD, in order to represent the swirling flow from a floor-mounted circular diffuser, the floor opening is divided into nine square cells. Each cell except the one in the middle has a different supply airflow direction and is in charge of one eighth of the total supply rate. The angle between the supply airflow and the floor is 30^0. Detailed descriptions of this treatment are given in Gao and Niu (2007).

Two physiological activities are taken into account: a steady exhalation process and one transient sneezing process. The real-body-shaped manikin in the computational domain provides both nose and mouth openings. Previous studies (Qian et al. 2006, Bjorn and Nielsen 2002) found that the exhaled air conditions (exhalation direction,

velocity, etc) from the source index patient have a major effect on the personal exposure and indoor concentration contours. Here, the dynamic respiration cycle is simplified by a steady exhalation process through both nostrils. The exhaled air is continuously impelled out 45^0 downwards from the nostrils at a rate of 8.4 l/min and a temperature of 35℃. 8.4 l/min corresponds to the breathing rate of an adult in a metabolic level during general office works. According to the PIV measurement by Zhu et al. (2006), the sneezed airflow spurts out 45^0 downwards from the nose at a velocity of 22 m/s. The sneezing process lasts 0.5 s.

Airflow simulation

The non-isothermal three-dimensional airflow is modeled using the RNG k-ε model. This model is reasonably accurate for a wide range of turbulent flows in the engineering field. The general form of the governing equations is as follows:

$$\frac{\partial(\rho\phi)}{\partial t} + div\left(\rho\vec{U}\phi\right) = div\left(\Gamma_\phi grad\phi\right) + S_\phi \tag{1}$$

Table 2 lists the diffusion coefficients and source terms for different scalar qualities. Two specialties in RNG k-ε model are the derivation of effective viscosity μ_{eff} and strain rate term R_ε in the ε equation. μ_{eff} is calculated by a differential equation:

$$d\left(\frac{\rho^2 k}{\sqrt{\varepsilon\mu}}\right) = 1.72\frac{\hat{v}}{\sqrt{\hat{v}^3 - 1 + C_v}}d\hat{v} \tag{2}$$

where $\hat{v} = \mu_{eff}/\mu$, $C_v = 100$. Equation (2) allows the model to better handle the low-Reynolds-number flows and near-wall flows since the indoor airflow is usually not fully turbulent. The term R_ε makes the RNG k-ε model more responsive to the effects of rapid strain and streamline curvature than the standard k-ε model. The buoyancy term is included in the y direction momentum equation, k and ε equation. Air density is defined as a function of its temperature by a piecewise-linear relationship. In the transient simulation of sneezing, the time step during 0.5 s sneezing process is 0.002 s. This is small enough to ensure the Courant number less than 1.0. After sneezing ends, the time step is gradually increased to 0.05 s to speed the calculation.

To compare the dispersion characteristics of gaseous pollutants and expiratory aerosols, the tracer gas, CO_2, with a 5% mass fraction, is added into the exhaled air. The species transport equation (as shown in Table 2) is solved together with the momentum and energy equations.

The grid independence is tested with two mesh sizes although strict check is not implemented by using the grid convergence index (GCI). The results for 500,000 and

750,000 are similar in term of velocity, temperature, turbulent kinetic energy, and dissipation rate distributions.

Particle modeling

The expiratory aerosol sizes have a wide spectrum from O(1μm) to O(1000μm) (Nicas et al. 2005). But when these droplets are introduced into the air, they quickly shrink by about 50% in diameters by evaporation. Most of the droplet nuclei fall in the size range of O(1~10μm) (Morawska et al. 2008). Droplets less than 10.0 μm can reach the alveolar region with a different efficiency, posing an infection risk for a susceptible person (Hinds 1999). Thus we simulated 1μm, 5μm, and 10μm droplet nuclei. The evaporation process is ignored because it is instantaneous compared with the time scale of airflows and particle movements (Nicas et al. 2005).

The airborne particles in indoor air can be deemed as dilute systems because the concentration is usually lower than 10^8 particles per m^3. This feature indicates that one-way coupling in the simulation is rational. The coagulation effect could be ignored since a significant change in particle number caused by coagulation may need more than several days, which is much longer than the characteristics time of the indoor air flow. In the present modeling of droplets, both the fluid phase and the particulate phase are treated as interpenetrating continua. But there are drift fluxes between them, which is caused by gravitational setting. Therefore a gravity vector is added into the convection term of the governing equation for droplet transport:

$$\frac{\partial(\rho C)}{\partial t} + \nabla \bullet (\rho(\vec{U} + \overrightarrow{V_S})C) = \nabla \bullet \left[\rho\left(D_p + \varepsilon_p\right)\nabla C\right] + S_C \qquad (3)$$

The gravitational settling velocity of particles ($\overrightarrow{V_S}$) is calculated by Stokes equation (Hinds 1999). For particles with very small relaxation time, particle eddy diffusivity ε_p approximates the carried fluid turbulent diffusivity ν_t (Hinze 1975). For 1.0μm particles, Bownian diffusion coefficient D_p, i.e. 2.9×10^{-11} m^2/s, is much weaker than kinetic viscosity and the turbulent diffusion coefficient. Therefore, in Equation 3, $\rho\left(D_p + \varepsilon_p\right)$ is replaced by μ_{eff}.

Another mechanism of droplets differing from gaseous species is deposition at solid surfaces. Although the amount of deposited droplets is usually much smaller than that of droplets exhausted by ventilation, in buildings with low air exchange rate droplet deposition may also constitute a major removal process. Experimental study found the deposition rate coefficient varied with intensity of air movement and with the level of room furnishing within the range of 0.10-0.38 h^{-1} for 0.5-1.0μm particles (Thatcher et al. 2002). For 10.0μm particles, given the current surface-to-volume ratio of 2.16 m^{-1}, the loss rate caused by deposition could be as high as 3.5 h^{-1}, which is comparable to the air change rate. To quantify the deposition amount and to close Equation (3) at

wall surfaces, we adopt the L&N deposition model (Lai and Nazaroff 2000). With the assumption that the deposition flux is one-dimensional and constant in the concentration boundary layer, the L&N model integrates Fick's law across the boundary layer and expresses the dimensionless deposition velocity as a function of droplet properties and local airflow conditions. The drift-flux model combined with wall treatment using the L&N model has been validated against two sets of experimental data in our previous study (Gao and Niu 2007).

Evaluation index

In the steady conditions, normalized concentration values at some interested locations are inspected to assess the performance of air distribution types. The concentrations are non-dimensioned by the value at the nose. In the transient conditions where sneezed droplets disperse as time elapses, two issues may be crucial: the droplet cloud gravity center (CGC) point and the droplet cloud spatial volume (CSV) in which the concentration is higher than a fixed value, i.e. infection threshold. In a room, CGC indicates the polluted location and CSV shows how large the polluted zone is. In the drift-flux model, determination of CSV is achieved by labeling each computational cell by a new variable, which is 1.0 if the concentration in this cell is higher than or equal to the infection threshold, otherwise 0. Then CSV can be acquired by integrating this variable across the computational domain. However, determination of CGC in the frame of Eulerian approach is not an easy job although it is simpler in Lagrangian method.

3. Results and discussion

Airflow fields

The airflow patterns and temperature profiles are shown in Figure 3. The mean temperature at the middle height (1.4m) is 23℃ in all ventilation systems although the supply air temperature is 2℃ lower in MV. As expected, forced convection in MV drives the well-mixing of air and heat, while natural convection produces temperature gradients in DV and UFAD. Natural convection at the human body is of special interest since it interacts with the respiration flows. Close inspect on the upward air speed above the human head finds that the maximum speed is 0.30m/s, 0.14m/s, and 0.18m/s in MV, DV, and UFAD, individually. The warm plume surrounding the body is the strongest in MV.

Steady state simulations

Figure 4 illustrates the concentrations in the middle section (Y=1.5m) of the room. The distribution of CO_2 and 10.0μm droplets shows similar patterns. In MV, exhaled air is drawn upward by the buoyancy forces while in DV and UFAD exhaled air is locked horizontally in the breathing height. Due to the relatively weak momentum of the exhaled air jet from normal respiration, the dispersion of the exhaled droplets is controlled by the combined effect of room airflows, exhaled airflow, and the warm

thermal plume around the body. In DV and UFAD, the vertical temperature gradient restrains the development of the natural convection at the body surface. Thus the upward convective airflow is not as strong as that in MV where the exhaled air is entrained up by the body plumes. Figure 5 shows the average values of normalized concentrations in horizontal planes across the room at different height level. The droplets are well mixed in MV. But in DV and UFAD, the highest concentration appears in the height between 1.2~1.5m (Note that the height of the nose is about 1.35m). This middle-height-pollution effect disobeys the general two-zone understanding of DV that there is a clean zone in the lower level and a polluted zone in the upper level in a room.

This finding is in line with the experimental results by Qian et al. (2006). In their experiments, two manikins lie on two beds in a hospital ward with mixing, downward, and displacement ventilation. Using N_2O as a representative of droplet nuclei, both the smoke visualization and the concentration distribution indicate that exhaled jet from a lying person penetrates a short distance and is diluted quickly into the room air. For DV, the exhaled jet penetrates a longer distance, exhibiting a high concentration layer in certain heights. The present study implies that this phenomenon of tracer gases may also be true for respiratory particles smaller than 10.0μm.

In our previous study (Gao and Niu 2007), particles are uniformly released at the surface of the heat source (item 2 in Figure 2) without initial momentums at a rate of 0.154 ug/s. For 5.0 μm particles, the body inhaled concentration in MV, DV, and UFAD is 2.17, 1.50, and 1.68ug/m^3, respectively, and for 10.0μm particles, 1.02, 1.40, 1.88ug/m^3, respectively. In that case, as a particle source is combined with the heat source, particles smaller than 5.0μm behaves like tracer gases with a higher ventilation efficiency in the stratified thermal environments than in the uniform environments. However, particles larger than 10.0μm are too heavy to be carried upwards by the buoyancy effect. They linger in the breathing height, causing a higher exposure than in MV. Therefore, the performance of DV and UFAD is particle-size sensitive if the particulate matter is produced in heat plumes. Friberg et al. (1996)'s experiments in an operating theatre proved that DV was less effective with regard to remove large particle (>10.0μm) because the upward airflow in DV may not be sufficient to transport large particles up to the ceiling exhaust. In the present study, for both tracer gases and particles, a maximum concentration in the breathing height in DV and UFAD appears. It appears that, with the current setting of indoor furniture and ventilation rate, MV tends to generate a uniform concentration distribution while, in DV and UFAD, exhaled pollutants from occupants are trapped in the breathing zone.

The 'trap' phenomenon of expiratory pollutants in the thermally stratified environments is undesirable with regard to the control of cross-infections of respiratory diseases. Locally gathered respiratory droplets in the breathing zone can increase the infection risk. How to resolve this problem may be closely linked with

the possibilities of elevating the trap layer above the occupied zone. The location of the trap layer is believed to be affected by the air change rate and the thermal conditions, and a more in-depth parametric study is necessary.

Transient simulations

Figure 6 shows the dynamic dispersion process in the first 6s. The sneezed air impinges at the desk, is blocked by the computer, and then diverges into two sides. High speed sneezed/coughed airflow shows a feature of orientation. The spatial relationship among indoor furniture and occupants significantly influence the transport of saliva droplets. The 'target zone' of the sneezed/coughed jet flow is of high infection risk. Keeping a certain distance between occupants and masking the nose/mouth when sneezing/coughing are foreseeable measures to reduce the airborne disease transmissions.

The dilution process of the aerosol cloud is illustrated in Figure 7. The sneezed droplets are diluted by the room air most quickly in MV. For example of 10.0μm droplets being diluted to one ten thousandth, the maximum polluted volume and its corresponding time is 4.3m^3 and 20s in MV, 4.0m^3 and 55s in DV, and 3.2m^3 and 40s in UFAD, respectively. The droplet cloud is diluted quickly in MV, but slowly in DV. Here for one sneez, 1:10000 dilution of the sneezed droplet concentration has a volume at the order of magnitude of the room space, warning a serious infection condition if the infection threshold is 0.0001 or below, not to mention that people may sneeze/cough repeatedly. The quick dilution in MV is a two-edge sword. It can rapidly dilute the concentration below the infection threshold; also can fast transport the droplets to a further distance to cause infection if the threshold is very low. Given a disease whose infection threshold is 0.0001, at 20s after the beginning of sneezing, the dangerous zone where concentration is higher than 0.0001 in MV is 4.3m^3. It is 2.5m^3 in DV and 2.3m^3 in UFAD. However, at 60s, the room space with MV is safe whereas even at 100s the indoor air in DV or UFAD is still infectious.

In some studies, mixing time is defined as the shortest time required to reach a well-mixing condition (Abadie and Liman 2007). Well-mixing is characterized by two requirements: the length scale of the droplet cloud is comparable with the room length scale and the standard deviation of the concentration should be below 10% of the arithmetic mean concentration. For a point pulse release of pollutants like sneezing or coughing, well-mixing conditions may not be achieved before the pollutants are ventilated out. By validation against their experiments, Gadgil et al. (2003)'s simulation found the mixing process depends primarily on the mean airflow in the room, and secondarily on the pollutant source location. This finding accords with the results in Figure 7. Examination of the air speed in the breathing height shows a mean value of 0.1m/s in MV, which is about one time higher than that in DV and UFAD. It reminds us the importance of indoor air speed levels in the control of cross-infections although the air change rate is the same. High speed assists droplet dispersion. Low speed could cause a local accumulation of droplets over a long time period.

4. Conclusions

This study adopts Eulerian method to investigate the spatial concentration distribution and temporal evolution of exhaled and sneezed droplets within the range of 1.0~10.0μm. Special attention is paid in comparing the performances of three common ventilation types, i.e. mixing ventilation, displacement ventilation, and under-floor air distribution in their abilities to reduce cross-infection risks. The simulation of a real-life office well represents the typical airflow and temperature distributions in MV, DV, and UFAD. The important conclusions are as follows.

1. Respiratory droplets smaller than 10.0μm disperse like tracer gases. In steady conditions, the exhaled droplets from normal breathing process can be trapped at a certain height level in DV and UFAD, resulting in a maximum droplet concentration in the breathing height and indicating a higher infection risk.
2. In DV and UFAD, the distribution characteristics of particulate matters generated from a surface with convective heat, and from human nose are entirely different, and the trapped layer appears when the pollutants are released from the latter.
3. Transient dilution of sneezed/coughed droplets is primarily dominated by the indoor air velocities in the breathing zone. The higher velocity level with MV makes the droplet cloud mix faster with the ventilation air than with DV and UFAD. Thermal stratification combined with the lower air velocity at the middle height can cause longer residence time of the respiratory droplets, thus potentially increase the exposure in the breathing zone.

The preliminary conclusion is that the trap-layer phenomenon of the respiratory droplets seems different from the two-zone theory of DV. More studies are needed to understand the influences of air change rate and the thermal conditions, and the resultant exposure with multiple occupants.

Acknowledgements

The project is funded by the Dean's reserve of Faculty of Construction and Land Use, The Hong Kong Polytechnic University.

References

1. Abadie MO, Liman K (2007). Numerical evaluation of the particle pollutant homogeneity and mixing time in a ventilated room. *Building and Environment*, 42: 3848-3854.
2. Bjorn E, Nielsen PV (2002). Dispersal of exhaled air and personal exposure in displacement ventilated rooms. *Indoor Air*, 12: 147-164.
3. CDC (1994). Guidelines for preventing the transmission of Mycobacterium tuberculosis in health-care facilities. Atlanta, GA: US Department of Health and Human Services, Public Health Service, Centers for Disease Control and Prevention.
4. Chao CYH, Wan MP, To GN (2008). Transport and removal of expiratory droplets in hospital ward environment. *Aerosol Science and Technology*, 42: 377-394.

5. Friberg B, Friberg S, Burman LG, Lundholm R, Ostensson R (1996). Inefficiency of upward displacement operating theater ventilation. *Journal of Hospital Infection*, 33: 263-272.
6. Gadgil AJ, Lobscheid C, Adadie MO, Finlayon EU (2003). Indoor pollutant mixing time in an isothermal closed room: an investigation using CFD. *Atmospheric Environment*, 37: 5577-5586.
7. Gao NP, Niu JL (2007). Modeling particle dispersion and deposition in indoor environments. *Atmospheric Environment*, 41: 3862-3876.
8. Hinds WC (1999). Aerosol technology: properties, behavior, and measurement of airborne particles. John Wiley & Sons, Inc.
9. Hinze JO (1975). Turbulence. 2nd edition, New York, McGraw-Hill.
10. Hsu DJ, Swift DL (1999). The measurement of human inhalability of ultralarge aerosols in calm air using manikins. *Journal of Aerosol Science*, 30(10): 1334-1343.
11. Lai ACK, Cheng YC (2007). Study of expiratory droplet dispersion and transport using a new Eulerian modeling approach. *Atmospheric Environment*, 41: 7473-7484.
12. Lai ACK., Nazaroff WW. (2000) Modeling indoor particle deposition from turbulent flow onto smooth surfaces. Journal of Aerosol Science, Vol. 31, no. 4, pp. 463-476.
13. Li YG, Leung GM, Tang JW, Yang X, Chao CYH, Lin JZ, Lu JW, Nielsen PV, Niu JL, Qian H, Sleigh AC, Su HJJ, Sundell J, Wong TW, Yuen PL (2007). Role of ventilation in airborne transmission of infectious agents in the built environment-a multidisciplinary systematic review. *Indoor Air*, 17: 2-18.
14. Morawska L, Johnson G, Ristoski Z, Hargreaves M, Mengersen K, Chao CYH, Wan MP, Li YG, Xie XJ, Katoshevshi D (2008). Droplets expelled during human expiratory activities and their origin. In: Proceedings of the 11th International Conference on Indoor Air Quality and Climate, August 17-22, Copenhagen, Denmark.
15. Nazaroff WW (2008). Inhalation intake fraction of pollutant from episodic indoor emissions. *Building and Environment*, 43(3): 269-277.
16. Nicas M, Nazaroff WW, Hubbard A (2005). Toward understanding the risk of secondary airborne infection: emission of respirable pathogens. *Journal of Occupational and Environmental Hygiene*, 2: 143-154.
17. Qian H, Li Y, Nielsen PV, Hyldgaard CE. Wong TW, Chwang ATY (2006). Dispersion of exhaled droplet nuclei in a two-bed hospital ward with three different ventilation systems. *Indoor Air*, 16: 111-128.
18. Sun W, Ji J, Li YG, Xie XJ (2007) Dispersion and settling characteristics of evaporating droplets in ventilated rooms. *Building and Environment*, 42: 1011-1017.
19. Thatcher TL, Lai ACK, Moreno-Jackson R, Sextro RG, Nazaroff WW (2002). Effects of room furnishings and air speed on particle deposition rates indoors. *Atmospheric Environment*, 36(11): 1811–1819.

20. Xie X, Li YG, Chwang TY, Ho PL, Seto WH (2007) How far droplets can move in indoor environments-revising the Wells evaporation-falling curve. *Indoor Air*, 17(3): 211-225.
21. Zhao B, Zhang Z, Li XT (2007) Numerical study of the transport of droplets or particles generated by respiratory system indoors. *Building and Environment*, 40(8): 1032-1039.
22. Zhu SW, Kato S, Yang JH (2006). Study of transport characteristics of saliva droplets produced by coughing in a calm indoor environment. *Building and Environment*, 41(12): 1691-1702.

Tables

Table 1 The details of numerical methods

Turbulence Model	Renormalization k-ε model
Wall treatment	Non-slip, standard logarithmic wall function
Numerical Schemes	Upwind second order difference for the convection term; central difference for the diffusion term with second order accuracy; SIMPLEC algorithm
Window	Uniform heat flux 150W
Floor, ceiling, walls	Adiabatic wall
Vertical heat source	Uniform heat flux 100W
Human body	Fixed skin temperatures at 31℃
Computer	Uniform heat flux 120W
Desk	Adiabatic
MV inlet	Airflow rate 51l/s, turbulence intensity 20%, turbulence length scale 0.005m, temperature 17℃
DV inlet	Airflow rate 51l/s, turbulence intensity 15%, turbulence length scale 0.005m, temperature 19℃
UFAD inlet	Airflow rate 51l/s, turbulence intensity 15%, hydraulic diameter 0.07m, temperature 19℃
MV/DV/UFAD outlet	Velocity and temperature: free slip
Nose	For steady exhalation, respiration rate 8.4 l/min, exhaled air temperature 35℃, turbulence intensity 10%, hydraulic diameter 0.01m; For sneezing simulation, air velocity 22m/s, duration 0.5s.

Table 2 Diffusion terms and source terms in the governing equations

Item	Variable	Γ_ϕ	S_ϕ
continuity	1	0	0

x velocity	u	$\mu_{eff} = \mu + \mu_t$	$-\frac{\partial P}{\partial x} + \frac{\partial}{\partial x}\left(\mu_{eff}\frac{\partial u}{\partial x}\right) + \frac{\partial}{\partial y}\left(\mu_{eff}\frac{\partial v}{\partial x}\right) + \frac{\partial}{\partial z}\left(\mu_{eff}\frac{\partial w}{\partial x}\right)$
y velocity	v	$\mu_{eff} = \mu + \mu_t$	$-\frac{\partial P}{\partial y} + \frac{\partial}{\partial x}\left(\mu_{eff}\frac{\partial u}{\partial y}\right) + \frac{\partial}{\partial y}\left(\mu_{eff}\frac{\partial v}{\partial y}\right) + \frac{\partial}{\partial z}\left(\mu_{eff}\frac{\partial w}{\partial y}\right) - \rho g$
z velocity	w	$\mu_{eff} = \mu + \mu_t$	$-\frac{\partial P}{\partial z} + \frac{\partial}{\partial x}\left(\mu_{eff}\frac{\partial u}{\partial z}\right) + \frac{\partial}{\partial y}\left(\mu_{eff}\frac{\partial v}{\partial z}\right) + \frac{\partial}{\partial z}\left(\mu_{eff}\frac{\partial w}{\partial z}\right)$
kinetic energy	k	$\alpha_k \mu_{eff}$	$G_k + G_B - \rho\varepsilon$
dissipation rate	ε	$\alpha_\varepsilon \mu_{eff}$	$C_{1\varepsilon}\frac{\varepsilon}{k}\left(G_k + C_{3\varepsilon}G_B\right) - C_{2\varepsilon}\rho\frac{\varepsilon^2}{k} - R_\varepsilon$
temperature	T	$\frac{\mu}{\mathrm{Pr}} + \frac{\mu_t}{\sigma_T}$	S_T
concentration	C	$\frac{\mu}{Sc} + \frac{\mu_t}{\sigma_c}$	S_C

Note to Table 2

$G_k = \mu_t S^2$, $S = \sqrt{2S_{ij}S_{ij}}$, $S_{ij} = \frac{1}{2}\left(\frac{\partial u_j}{\partial x_i} + \frac{\partial u_i}{\partial x_j}\right)$, $G_B = \beta_T g \frac{\mu_t}{\sigma_T}\frac{\partial T}{\partial y}$,

$\mu_t = \rho C_\mu \frac{k^2}{\varepsilon}$, $C_\mu = 0.0845$, $C_{1\varepsilon} = 1.42$, $C_{2\varepsilon} = 1.68$, $C_{3\varepsilon} = \tanh\left|\frac{v}{\sqrt{u^2 + w^2}}\right|$,

$\sigma_T = 0.85$, $\sigma_C = 0.7$,

$\alpha_k = \alpha_\varepsilon$ is calculated by $\left|\frac{\alpha - 1.3929}{\alpha_0 - 1.3929}\right|^{0.6321}\left|\frac{\alpha + 2.3929}{\alpha_0 + 2.3929}\right|^{0.3679} = \frac{\mu}{\mu_{eff}}$

where $\alpha_0 = 1.0$. If $\mu << \mu_{eff}$, then $\alpha_k = \alpha_\varepsilon \approx 1.393$

$R_\varepsilon = \frac{C_\mu \rho \eta^3 \left(1 - \eta/\eta_0\right)}{\left(1 + \beta\eta^3\right)} \times \frac{\varepsilon^2}{k}$, where $\eta = Sk/\varepsilon$, $\eta_0 = 4.38$, $\beta = 0.012$

Figure Captions

Figure 1 A paradigm of airborne infection process (The exposure figure is from Hsu and Swift (1999))

Figure 2 Configuration of the simulated office (room length (X) 4m, width (Y) 3m, height (Z) 2.7m; 1-window; 2-vertical heat source; 3-computer; 4-table; 5-human

body; 6-mixing ventilation inlet $0.2\text{m}\times0.1\text{m}$; 7-displacement ventilation outlet $0.4\text{m}\times0.3\text{m}$; 8-mixing ventilation outlet $0.4\text{m}\times0.3\text{m}$; 9-displacement ventilation inlet $0.4\text{m}\times0.5\text{m}$; 10-UFAD inlet $0.21\text{m}\times0.21\text{m}$; 11-UFAD outlet $0.4\text{m}\times0.4\text{m}$)

Figure 3 Air flow patterns and temperature distributions in the middle section (Y=1.5m) of the room with (a) MV; (b) DV; (c) UFAD

Figure 4 Normalized concentration in the middle section (Y=1.5m) in the room with (a) MV, CO_2; (b) MV, 10.0μm droplets; (c) DV, 10.0μm droplets; (d) UFAD, 10.0μm droplets. The concentration in the exhaled air is denoted as 1.0.

Figure 5 Normalized concentrations at different height levels (a) MV; (b) DV; (c) UFAD. The concentration in the exhaled air is denoted as 1.0.

Figure 6 Contour of normalized concentration at 0.001 for 1.0μm particles at different times after the start of sneezing: (a) 0.5s; (b) 1.0s; (c) 3.0s; (d) 6.0s

Figure 7 Evolution of the sneezed aerosol cloud volume (a) MV; (b) DV; (c) UFAD. The legends indicate the concentration level. For example, '10.0μm>0.0001' means that, at any points in the volume, the normalized concentration of 10.0μm droplets is no less than 0.0001.

Figures

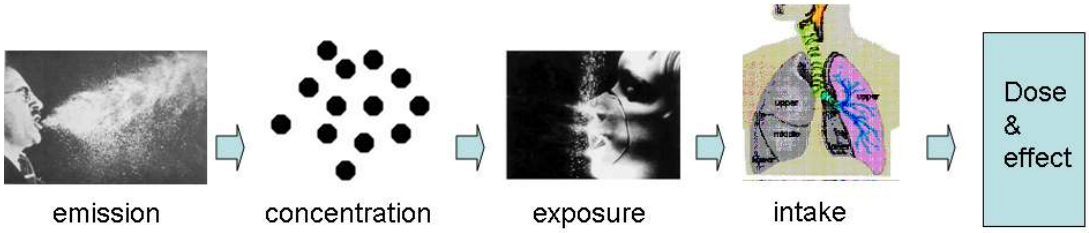

Figure 1 A paradigm of airborne infection process (The exposure figure is from Hsu and Swift (1999))

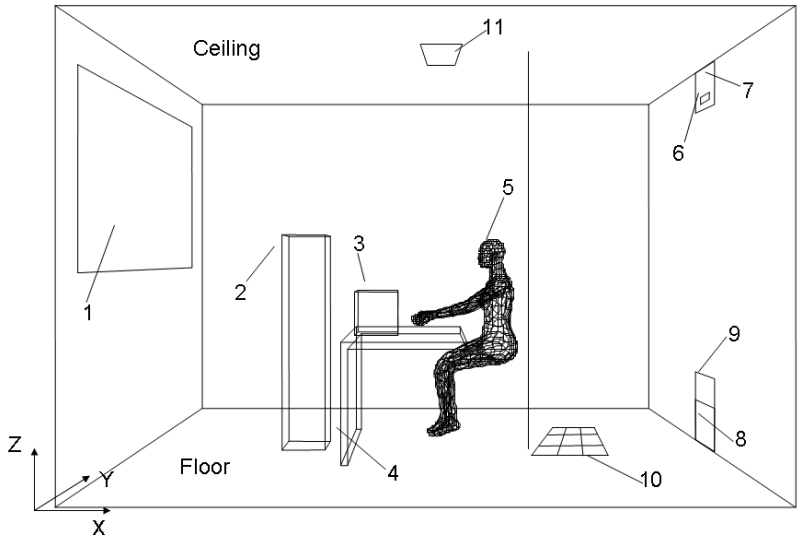

Figure 2 Configuration of the simulated office (room length (X) 4m, width (Y) 3m, height (Z) 2.7m; 1-window; 2-vertical heat source; 3-computer; 4-table; 5-human body; 6-mixing ventilation inlet $0.2\text{m}\times0.1\text{m}$; 7-displacement ventilation outlet $0.4\text{m}\times0.3\text{m}$; 8-mixing ventilation outlet $0.4\text{m}\times0.3\text{m}$; 9-displacement ventilation

inlet $0.4\text{m} \times 0.5\text{m}$; 10-UFAD inlet $0.21\text{m} \times 0.21\text{m}$; 11-UFAD outlet $0.4\text{m} \times 0.4\text{m}$)

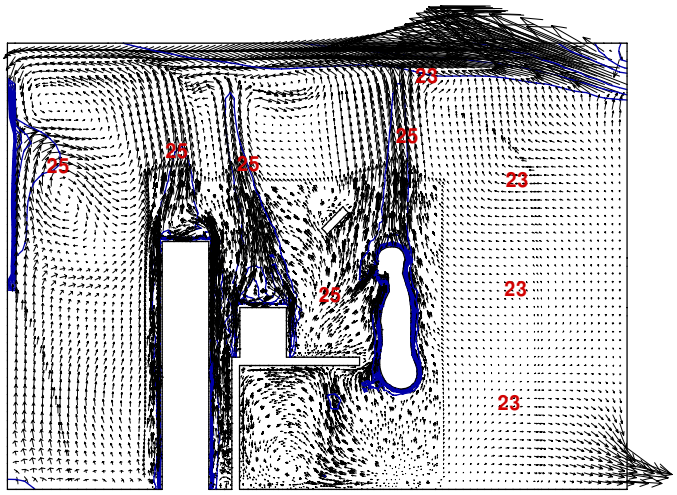

(a)

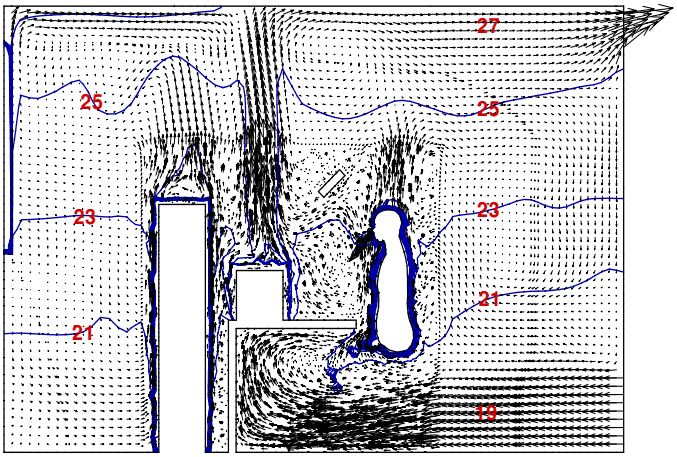

(b)

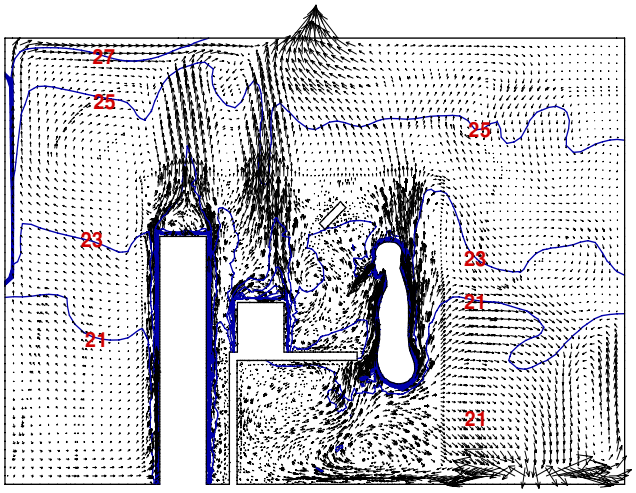

(c)

Figure 3 Air flow patterns and temperature distributions in the middle section (Y=1.5m) of the room with (a) MV; (b) DV; (c) UFAD

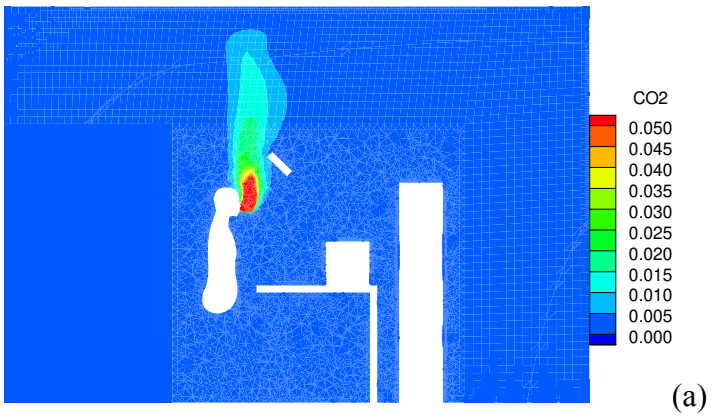

(a)

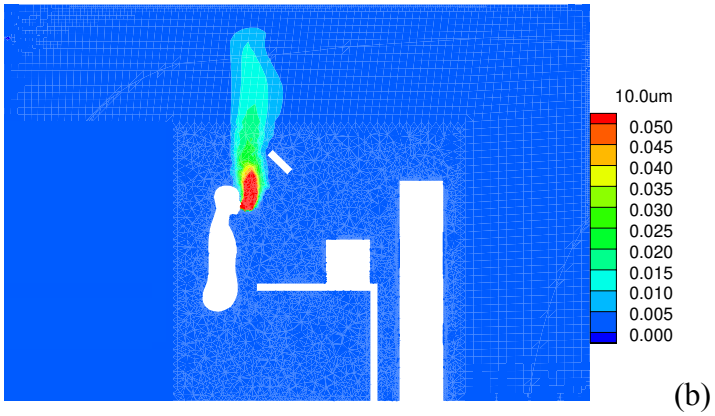

(b)

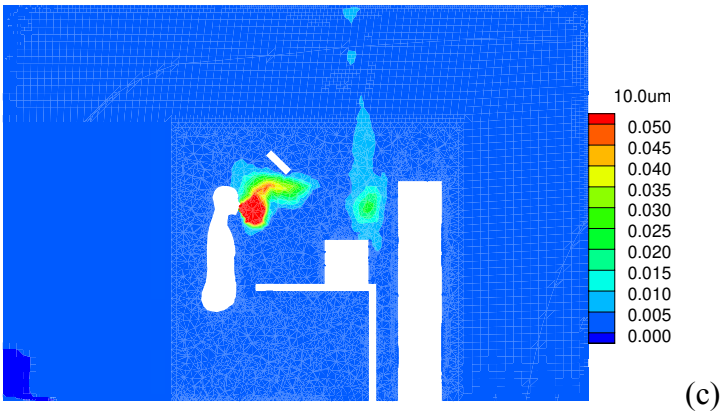

(c)

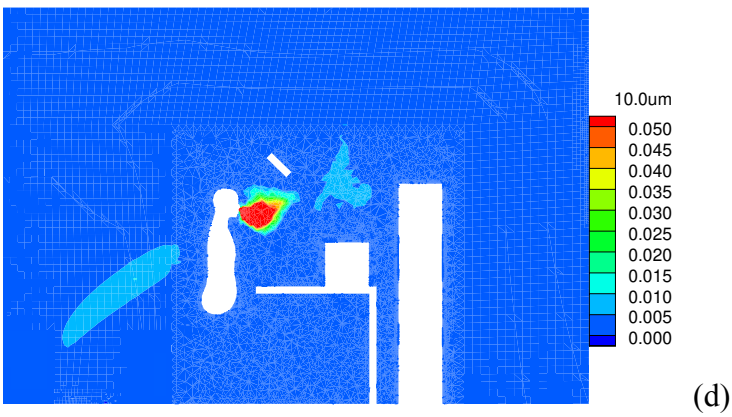

(d)

Figure 4 Normalized concentration in the middle section (Y=1.5m) in the room with

(a) MV, CO_2; (b) MV, 10.0μm droplets; (c) DV, 10.0μm droplets; (d) UFAD, 10.0μm droplets. The concentration in the exhaled air is denoted as 1.0.

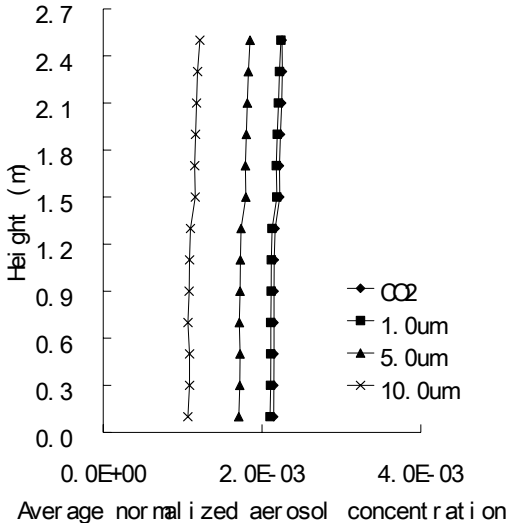

(a) MV

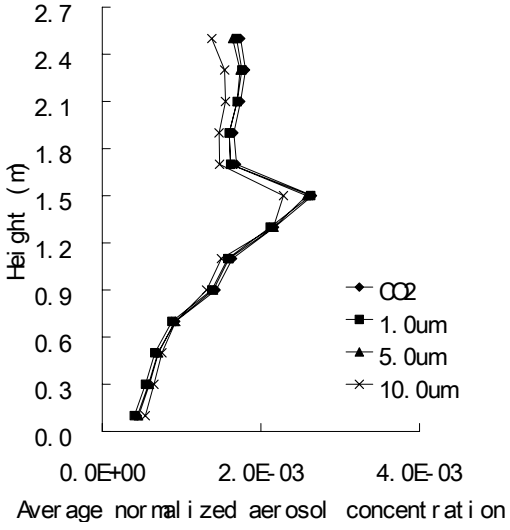

(b) DV

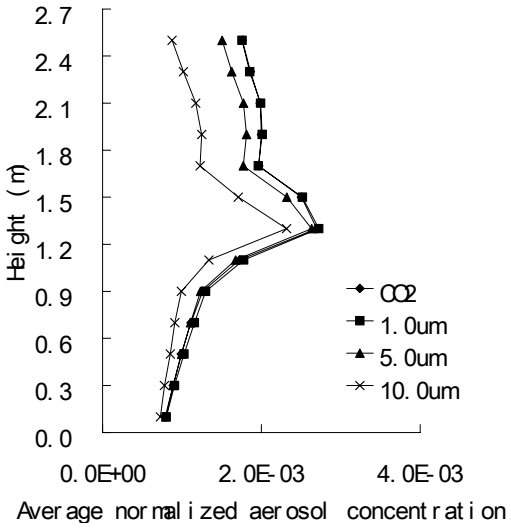

(c) UFAD

Figure 5 Average normalized concentrations in planes across the room at different height levels (a) MV; (b) DV; (c) UFAD. The concentration in the exhaled air is denoted as 1.0.

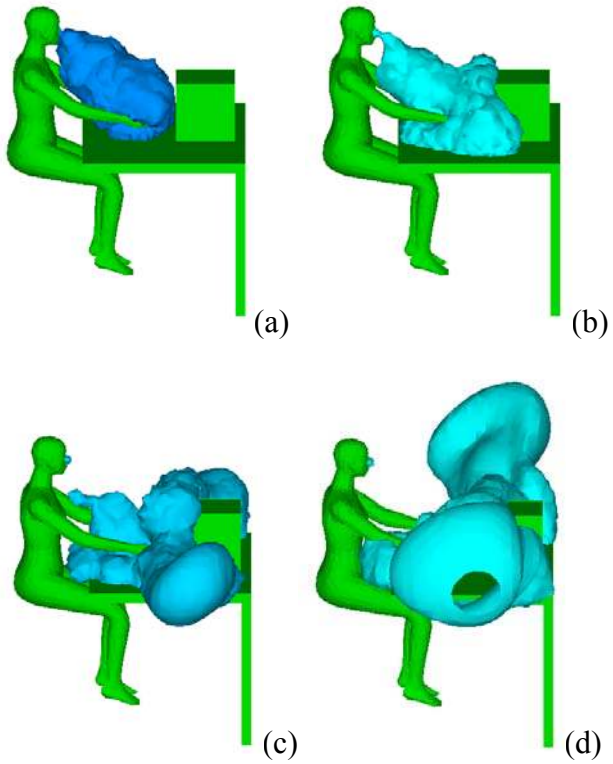

Figure 6 Contour of normalized concentration at 0.001 for 1.0μm particles at different times after the start of sneezing: (a) 0.5s; (b) 1.0s; (c) 3.0s; (d) 6.0s;

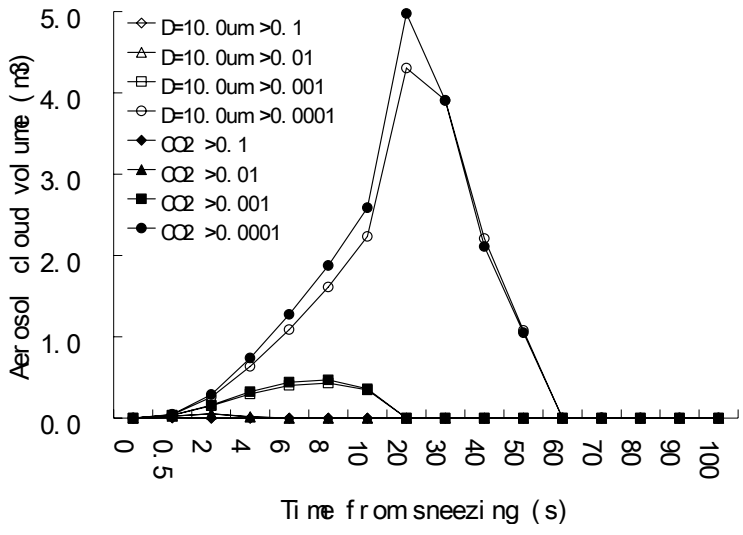

(a)

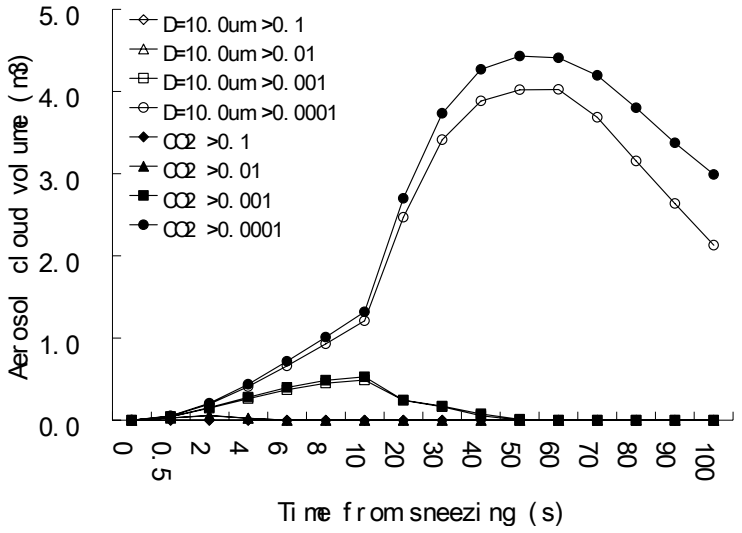

(b)

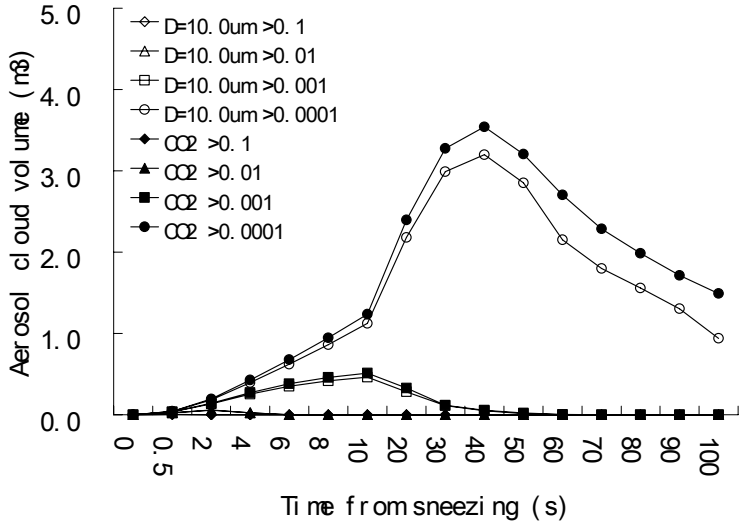

(c)

Figure 7 Evolution of the sneezed aerosol cloud volume (a) MV; (b) DV; (c) UFAD. The legends indicate the concentration level. For example, '10.0μm>0.0001' means that, at any points in the volume, the normalized concentration of 10.0μm droplets is no less than 0.0001.